

Design of a β -Ga₂O₃ Schottky Barrier Diode With p-type III-Nitride Guard Ring for Enhanced Breakdown

Saurav Roy, Arkka Bhattacharyya, and Sriram Krishnamoorthy

Abstract—This work presents the electrostatic analysis of a novel Ga₂O₃ vertical Schottky diode with three different guard ring configurations to reduce the peak electric field at the metal edges. Highly doped p-type GaN, p-type nonpolar AlGa_N and polarization doped graded p-AlGa_N is simulated and analyzed as the guard ring material, which forms a heterojunction with the Ga₂O₃ drift layer. Guard ring with non-polar graded p-AlGa_N with band gap larger than Ga₂O₃ is found to show best performance in terms of screening the electric field at the metal edges. The proposed guard ring configuration is also compared with a reported Ga₂O₃ Schottky diode with no guard ring and a structure with high resistive Nitrogen doped guard ring. The optimized design is predicted to have breakdown voltage as high as 5.3 kV and a specific on resistance of 3.55 m Ω -cm² which leads to an excellent power figure of merit of 7.91 GW/cm².

Index Terms—Ga₂O₃, Schottky barrier diode, guard ring, GaN, AlGa_N, Polarization doping, TCAD simulation.

I. INTRODUCTION

GALLIUM OXIDE (Ga₂O₃) has a huge potential for power device applications due to its high breakdown field. β -Ga₂O₃ has a band gap (4.6 eV) larger than GaN and SiC, with an estimated critical breakdown field as high as 8 MV/cm. Due to the large critical electric field, the Baliga Figure of Merit (BFOM) relevant to power switching could be 20003400 times that of Si, which is several times larger than that of SiC or GaN. Low doped drift layers in conjunction with large band gap materials can enable very high breakdown voltage. Various power devices using β -Ga₂O₃ have been demonstrated recently with high breakdown voltage in the vertical geometry. [1]–[12].

Several field management techniques have been explored for Schottky diodes over the years that includes edge terminations, superjunctions etc. Guard ring is one such edge termination technique where the anode metal edge is surrounded by a doped region with opposite polarity to that of the drift region to screen the high electric field generated at the metal edge. Lin et. al. [13] recently demonstrated a Schottky barrier diode (SBD) with nitrogen ion implanted guard ring (GR) with a maximum breakdown voltage of 1.43 kV. Zhou et. al. [14] also demonstrated a Ga₂O₃ SBD using Mg ion implanted guard ring with a breakdown voltage of 1.65 kV. A similar design with Argon implanted edge termination have also been reported by Gao et. al. [15]. Although these devices can

Saurav Roy, Arkka Bhattacharyya, and Sriram Krishnamoorthy are with the Department of Electrical and Computer Engineering, The University of Utah, Salt Lake City, UT, 84112, United States of America (e-mail: u1268405@utah.edu; a.bhattacharyya@utah.edu; sriram.krishnamoorthy@utah.edu).

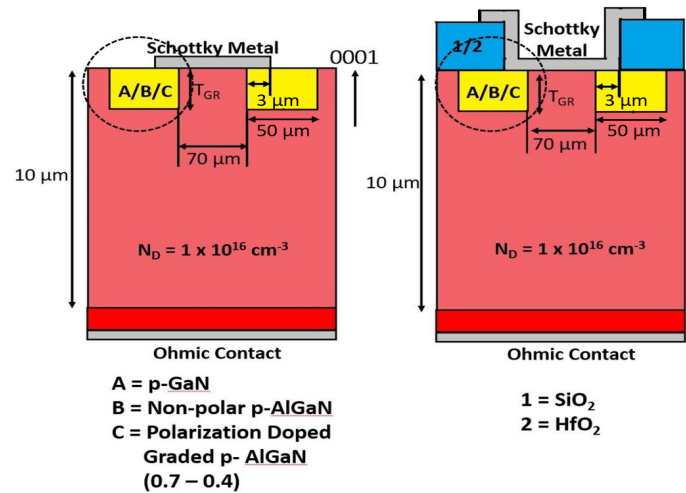


Fig. 1. Schematic of Ga₂O₃ SBD with guard rings (GR) where (A) Non-polar p-GaN GR (B) Non-Polar p-AlGa_N GR (C) Polarization doped graded p-AlGa_N GR with (1) SiO₂ (2) HfO₂ as field plate oxide.

achieve a breakdown improvement compared to the case with no guard rings, the lack of electric field screening due to the absence of carriers in the guard ring limits the breakdown voltage. A high resistive guard ring, as demonstrated in the previous devices can spread the depletion region and can reduce the field crowding at the metal edges. However, a guard ring with mobile holes can be very effective in screening the electric field at the metal edges due to the presence of a quasi neutral region and can dramatically shift the high field region from the metal edge to deep inside the device, thereby eliminating the effect of surface states which causes premature breakdown. Because of the difficulty in having hole concentration in β -Ga₂O₃ due to the absence of a shallow acceptor and hole self trapping, p-doped III-Nitrides would be a viable option to get a reasonably high hole concentration. The idea of heterostructure guard rings have been proposed on Silicon Carbide substrate previously [16]. Muhammed et. al. [17] have reported the growth of c-plane n-GaN epilayer on (2 0 1) β -Ga₂O₃ substrate using MOCVD. Vertical blue LEDs have also been demonstrated on (2 0 1) β -Ga₂O₃ substrates [18]. Shimamura et. al. [19] reported growth of c-plane GaN on (1 0 0) oriented β -Ga₂O₃ substrate using MOCVD. On the other hand Cao et. al. [20] reported the growth of non-polar a-plane GaN on (0 1 0) oriented β -Ga₂O₃ substrate by MOCVD. All these reports confirm the viability of growing electronic grade polar and non-polar GaN on β -

TABLE I
MATERIAL PARAMETERS

Material	Ga ₂ O ₃	GaN	AlN
Bandgap (eV)	4.85 [21]	3.3 [22]	6.2 [22]
Electron affinity (eV)	3.9 [21]	3.9 [22]	0.6 [22]
Relative permittivity	10 [21]	8.9 [23]	8.5 [23]
Electron Effective mass	0.28m ₀	0.22m ₀	0.4m ₀
Hole Effective mass	-	1m ₀	4m ₀
Critical Electric Field (MV/cm)	8 [21]	3.3 [23]	15 [23]
Sn Activation energy (eV)	0.13 [21]	-	-
Mg Activation energy (eV)	-	0.2 [23]	0.6 [23]
Spontaneous Polarization (C/m ²)	-	-0.034	-0.09

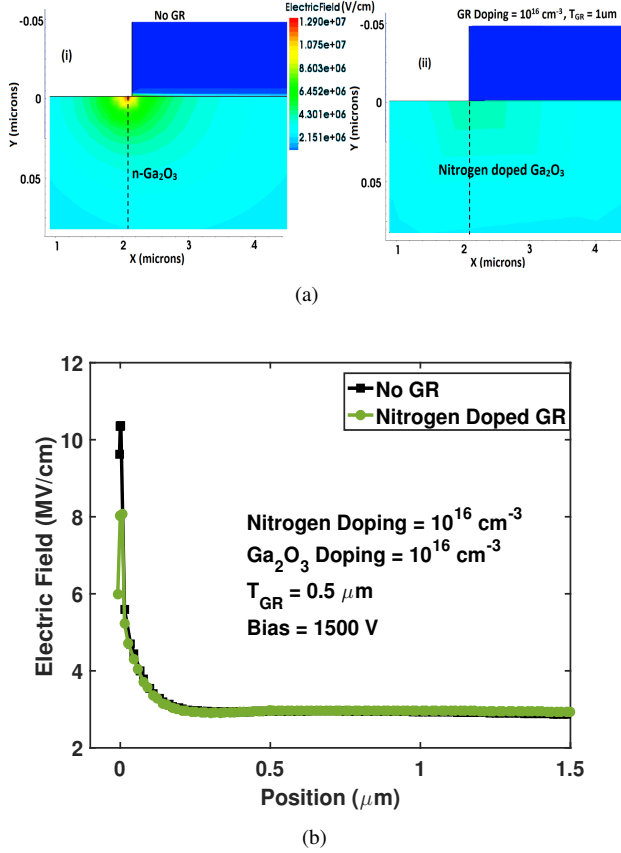


Fig. 2. (a) Electric field distribution in SBD for (i) no GR (ii) Nitrogen doped GR at bias voltage of 1500 V (b) Electric field vs position for N-doped GR and no GR at 1500 V along the cutlines shown in the contour plots.

Ga₂O₃ substrates depending on the choice of orientation of the substrate.

In this paper, we propose and design a Ga₂O₃ SBD with a p-doped III-Nitride guard ring using electric field simulations. We have explored three guard ring configurations including (i) p-Gallium Nitride (p-GaN) GR, (ii) Non-polar graded p-Aluminum Gallium Nitride (p-AlGa_{0.3}N) GR and a (ii) polar graded p-AlGa_{0.3}N GR. In this work we perform detailed electrostatic simulations to capture and manage high in III-nitride/ β -Ga₂O₃ heterostructures. The design is optimized to extract the optimum device parameters which efficiently reduces the electric field. We have also explored the additional use of field plate in the aforementioned optimum design to further minimize the peak electric field in the device structure.

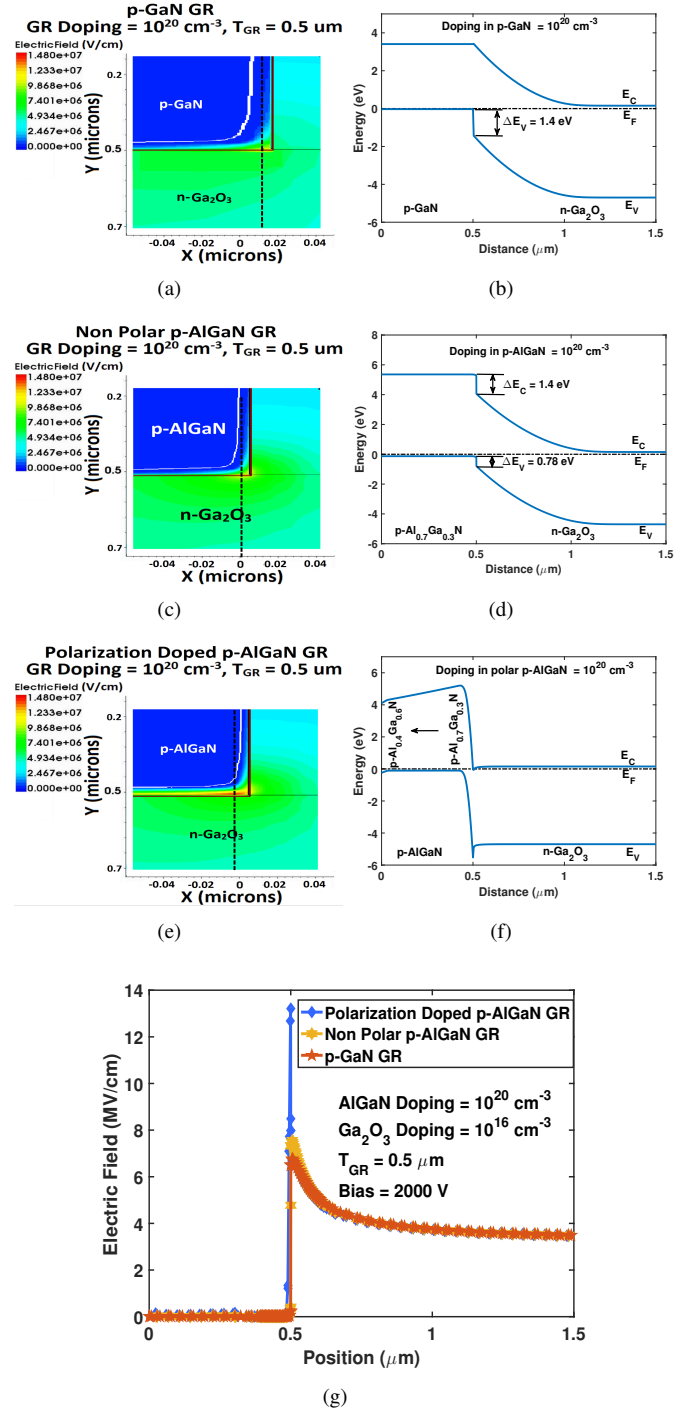


Fig. 3. Electric field distribution and equilibrium energy band diagram for SBD with (a) (b) non-polar p-GaN GR (c) (d) non-polar p-AlGa_{0.3}N GR (e) (f) polarization doped p-AlGa_{0.3}N GR respectively at bias voltage of 2000 V and GR doping of 10²⁰ cm⁻³ (g) Electric field vs position in SBD for the three different GR at 2000 V and at GR doping of 10²⁰ cm⁻³ along the cutlines shown in the contour plots.

II. SIMULATION METHODOLOGY

The schottky barrier diode device structure (Fig. 1) with varied guard ring thickness of T_{GR}, a 10 μm thick drift layer (N_D = 10¹⁶ cm⁻³), Ni/Au Schottky metal with a barrier height Φ_B of 1.4 eV [24], and a Schottky metal guard ring overlap of 3 μm is simulated using Sentaurus [25] 2D TCAD

device simulator. Width of the guard ring is considered to be $50 \mu\text{m}$. In the simulation, adequate numerical convergence was reached by an optimized meshing, with subnanometer grid spacing for the key electrical layers and their interfaces and larger spacings for drift region. Spontaneous polarization model is used to include polarization effect in the case of graded polar p-AlGaIn. The spontaneous polarization values of -0.034 and -0.09 C/m^2 is considered for GaN and AlN [23]. For p-type doping in GaN and AlGaIn, incomplete ionization model is also used to reflect the accurate hole concentration. In order to capture the accurate results for high doping case, Fermi-Dirac model is included for device operating biases. The device simulation setup uses well calibrated mobility model and thermodynamic transport model to match the recent experimental results [13]. The device breakdown voltage can be extracted from E-field simulation when the peak E-field reaches the GaN (3.3 MV/cm) or Ga_2O_3 (8 MV/cm) critical E-field. Band offsets were determined using electron affinity rule. The GaN/ Ga_2O_3 band offset estimated using electron affinity rule matches well with the experimentally determined band offsets [26]. The ionization integrals for avalanche breakdown were not evaluated in order to avoid excessive computation time. Furthermore, accurate ionization rate parameters are currently unknown for Ga_2O_3 . Hence it should be noted that the breakdown is not directly calculated, but can be estimated based on the generated electric field distributions [27]–[29]. It should also be noted that in real devices field crowding can also occur in the device corners. However those fields are always lower than the field crowding at the electrode edges which is the primary cause of device breakdown. Hence our comparison of device breakdown for the various configurations based on 2-D simulation is considerably reliable and was also demonstrated by other works [27]. All the material parameters for $\beta\text{-Ga}_2\text{O}_3$, GaN and AlN assumed in the device simulation are presented in Table I. All the other material parameters for intermediate Al compositions in $\text{Al}_x\text{Ga}_{1-x}\text{N}$ have been calculated based on GaN and AlN parameters using Vegard's law.

III. RESULTS AND DISCUSSIONS

The SBD with nitrogen doped GR and the one with no GR is simulated for comparison and the electric field profiles are shown in Fig. 2(a) (i) and (ii) respectively. The circled cross-section in Fig. 1 is magnified and shown for all the electric field contours. The bias voltage is taken to be 1500 V . Ionization energy of Nitrogen in $\beta\text{-Ga}_2\text{O}_3$ is considered to be 2 eV [30]. The maximum electric field is at the metal edge in both the cases and we can see that the field is reduced in the guard ring structure in Fig. 2(b) as expected and also experimentally reported [13].

We now explore the use of p-GaN as the guard ring material (Fig. 3(a)). The use of magnesium-doped GaN guard ring, enables screening of the electric field at the metal edges due to the presence of mobile holes. The activation energy for Mg in case of p-GaN is considered to be 0.2 eV [31]. The doping concentration is taken to be 10^{20} cm^{-3} (hole concentration = $8.2 \times 10^{18} \text{ cm}^{-3}$) and the guard ring thickness is $0.5 \mu\text{m}$ and the anode voltage is 2000 V . The peak electric field has

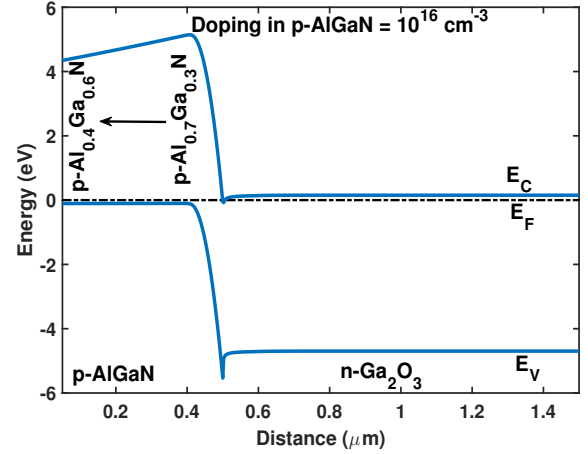


Fig. 4. Equilibrium energy band diagram of the simulated SBD with polarization doped p-AlGaIn GR for $T_{GR} = 0.5 \mu\text{m}$ and $N_D = 10^{16} \text{ cm}^{-3}$. Al composition is graded from 70 % to 40 % from the p-AlGaIn/n- Ga_2O_3 heterointerface to the SBD surface.

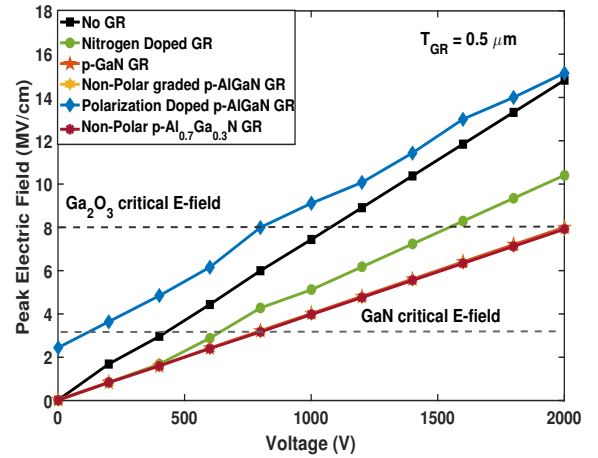


Fig. 5. Peak electric field vs applied bias in SBD for different GR configurations with $0.5 \mu\text{m}$ of GR thickness and 10^{20} cm^{-3} of GR doping.

now moved to the p-GaN/n- Ga_2O_3 heterojunction as can be seen in the electric field contour shown in Fig. 3(a). Fig. 3(b) shows the equilibrium energy band diagram of p-GaN/n- Ga_2O_3 heterojunction. At the anode bias of 2000 V , the peak electric field at the p-GaN/n- Ga_2O_3 heterojunction exceeds the critical field of GaN (3.3 MV/cm). We simulated the p-GaN guard ring configuration as a function of anode voltage and the results are presented in Fig 5. The breakdown voltage of the p-GaN guard ring configuration presented here is 750 V .

To be able to leverage the high critical E-field of $\beta\text{-Ga}_2\text{O}_3$, a better design would be to use a guard ring material with an enhanced critical field as compared to $\beta\text{-Ga}_2\text{O}_3$. So, we now study a graded p-AlGaIn guard ring with aluminum composition graded from 70 % at the AlGaIn/ Ga_2O_3 interface to 40 % at the SBD surface. Lower Aluminum content is employed closer to the surface so as to achieve higher mobile hole concentration. Fig. 3(c) shows the electric field distribution using graded AlGaIn for a doping concentration of 10^{20} cm^{-3} . However since the ionization energy of Mg is very

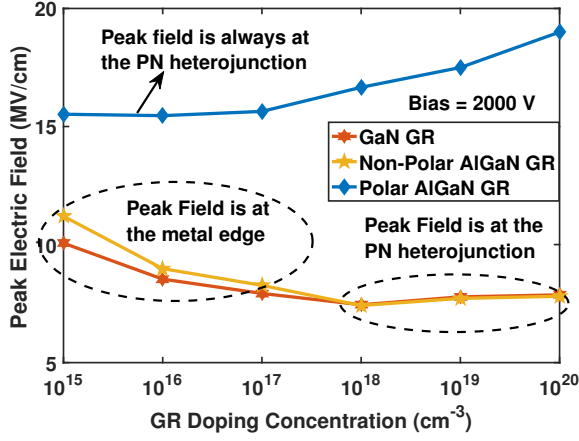


Fig. 6. Peak electric field vs GR doping concentration with $0.5 \mu\text{m}$ of GR thickness and at applied bias of 2000 V for different GR configurations.

high for AlGaN with high Al composition, it is very difficult to realize a high hole concentration. In fact for Mg concentration below 10^{18} cm^{-3} , the peak electric field is always at the metal edge because of the depletion of the entire GR. But if we grow c-axis oriented AlGaN with graded Al composition with decreasing Al composition from heterointerface to the surface, we can realize a 3-D slab of holes (3DHS) [32] due to the polarization doping effect. This is expected to significantly increase the hole concentration even with low Mg doping due to field ionization of dopants. Fig. 3(e) shows the electric field distribution in the polarization doped $\text{p-Al}_x\text{Ga}_{(1-x)}\text{N}$ (where $x = 70\%$ at the heterojunction to 40% at the SBD surface) GR. The hole concentration in this guard ring structure increased from the non-polar case by a significant amount (2×10^{17} to $6 \times 10^{18} \text{ cm}^{-3}$). Band diagram of the polarization-doped polar graded p-AlGaN guard ring configuration is shown in Fig. 3(f). It can be observed that the peak electric field is now at the heterojunction mainly due to the positive polarization sheet charge at the $\text{p-Al}_{0.7}\text{Ga}_{0.3}\text{N}/\text{n-Ga}_2\text{O}_3$ heterojunction. The energy bands fall rapidly at the polar p-AlGaN/n-Ga₂O₃ interface, thus increasing the electric field compared to the non-polar p-AlGaN/n-Ga₂O₃ interface as shown in Fig. 3(g). Even for the low doped case, the bands fall rapidly at the p-AlGaN/n-Ga₂O₃ heterointerface as shown in Fig. 4. So, a polarization doped p-AlGaN GR would serve no benefit in reducing the peak electric field.

Fig. 5 shows the peak electric field vs applied bias for SBD with the five different guard ring structures. The doping concentration for p-type guard ring is taken to be of 10^{20} cm^{-3} and for Nitrogen-doped case it is taken to be of 10^{16} cm^{-3} and the GR thickness is taken to be $0.5 \mu\text{m}$. The non-polar graded p-AlGaN, ungraded p-AlGaN, and p-GaN guard ring shows best performance in terms of reducing the peak electric field. However the SBD with GaN guard ring crosses its critical electric field of 3.3 MV at 750 V. The non polar $\text{p-Al}_x\text{Ga}_{1-x}\text{N}$ GR with uniform Al composition ($x = 60\%$) has a critical electric field as high as gallium oxide and hence the breakdown voltage can be as high as 2000 V as shown in the Fig. 5. The electric field is very high in case of the SBD with polarization doped AlGaN GR because of the high field

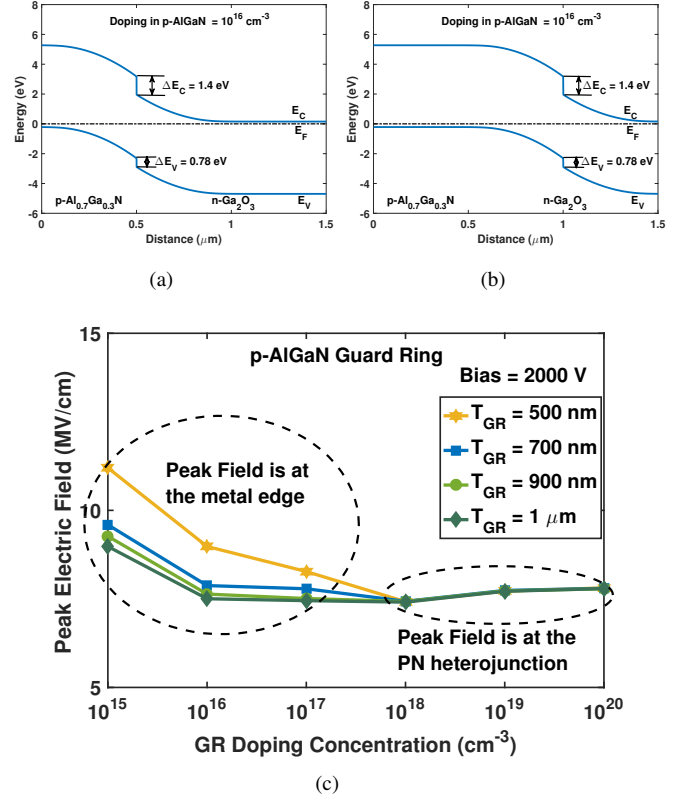


Fig. 7. Equilibrium energy band diagram of the simulated SBD with nonpolar p-AlGaN GR for (a) $T_{GR} = 0.5 \mu\text{m}$ (b) $T_{GR} = 1 \mu\text{m}$. Al composition is considered to be 70%. (c) Peak electric field vs GR doping concentration with non-polar AlGaN GR and at applied bias of 2000 V for different GR thicknesses.

at the heterointerface.

Doping and thickness of the guard ring are critical parameters that would determine the amount of electric field screening and location of the peak electric field. We simulated the three guard ring configurations excluding the SBD with no GR and nitrogen-doped GR, as a function of Mg doping for a fixed thickness of $0.5 \mu\text{m}$ at a bias of 2000 V. Doping in the guard ring is found to determine the location of the peak electric field as shown in Fig. 6. For the polar p-AlGaN guard ring, the peak electric field is always at the heterojunction irrespective of the doping. In the case of p-GaN and non-polar p-AlGaN guard ring, the peak field is at the metal edge for doping concentrations lower than 10^{18} cm^{-3} . Since a high GR doping is not necessary to minimize the peak field at the metal edge and since non polar graded and ungraded p-AlGaN GR shows similar performance, compositional grading in the GR is not required, which will mitigate the challenge involving growth of graded epitaxial layer of AlGaN inside the pocket of Ga₂O₃.

The electric field simulations clearly establish the comparably superior performance of non-polar p-AlGaN guard ring configuration. We now further focus on this particular configuration and study the effect of thickness of the guard ring. In the case of low-doped guard rings, in order to take advantage of holes, it is essential that the thickness must be sufficiently large to realize an undepleted region close to the metal. Equilibrium energy band diagram of non-polar graded

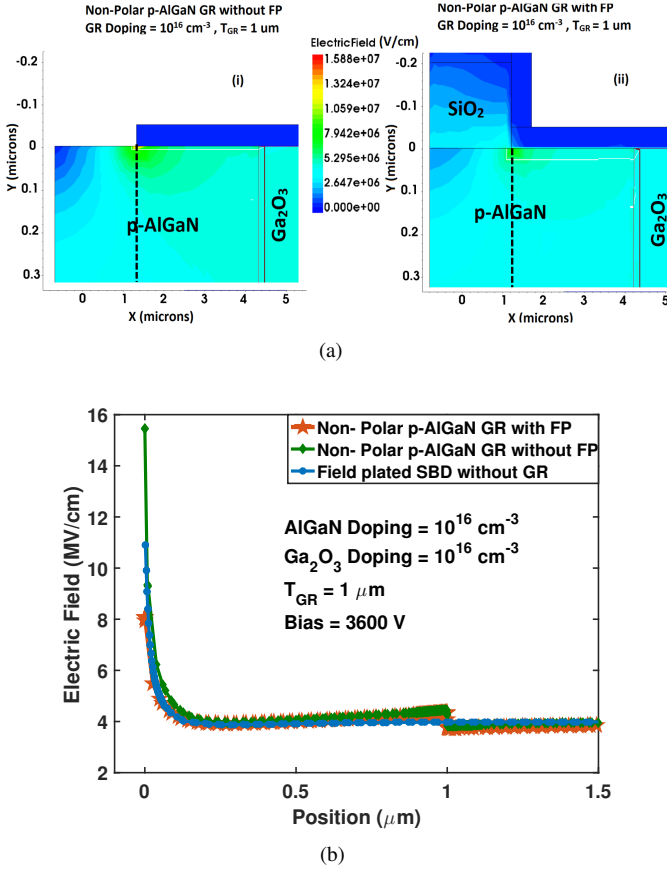


Fig. 8. (a) Electric field distribution in SBD for 1 μm thick non-polar AlGaIn GR (i) without field plate (ii) with field plate at bias voltage of 3600 V and GR doping of 10^{16} cm^{-3} (b) Electric field vs position for the two GR structure and also for field plated SBD with no GR at 3600 V and at GR doping of 10^{16} cm^{-3} along the cutlines shown in the contour plots.

p-AlGaIn GR with low doping (10^{16} cm^{-3}) with two different thicknesses is shown in Fig. 7(a) and Fig. 7(b). Presence of a quasi neutral region near the metal by employing a thick low doped guard ring (Fig. 7(b)) is expected to be beneficial for electric field screening. The quasi neutral region near the metal edge provides room for the growth of the depletion region at high reverse bias. The effect of guard ring thickness as a function of Mg doping is summarized in Fig. 7(c). The peak electric field at a bias of 2000 V can be reduced from 9 MV/cm to 7.5 MV/cm at a guard ring doping of 10^{16} cm^{-3} . The peak electric field reduces as the doping increases for doping concentration less than 10^{18} cm^{-3} . As the GR thickness increases, the peak electric field reduces till a doping concentration of 10^{17} cm^{-3} . Above this concentration the peak electric field shifts to the pn-heterojunction and the GR thickness has no effect on the peak electric field. In this regime, there is no advantage of using a field plate, since the peak field region is buried.

To further improve electric field management, we choose guard ring configuration B with a thickness of 1 μm and doping concentration of 10^{16} cm^{-3} . In this case, the peak electric field is at the metal edge. Now we analyze the potential for further improvement in breakdown voltage with a field plate. Fig. 8(a) shows the electric field distribution in the SBD

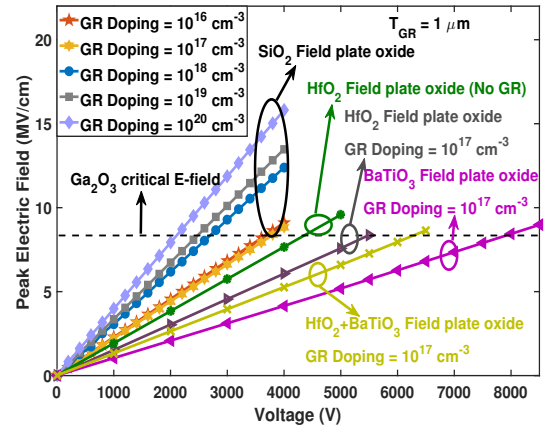


Fig. 9. Peak electric field vs applied bias in SBD with field plate and non-polar AlGaIn GR for different GR doping concentrations and with field plate oxides with different dielectric constants. Also compared with standard field plated SBD structure with no GR.

for a GR thickness of 1 μm and at a bias voltage of 3600 V (i) without and (ii) with a field plate respectively. An SiO_2 layer of 200 nm is used as the field plate oxide. We also compared our design with a field plated SBD without GR as shown in 8(b). The field plating has more impact on the reduction of the peak electric field compared to the SBD with only GR. However, SBD having a field plate combined with a thick p-AlGaIn GR dramatically reduces the peak electric field at the metal edge. Here again the peak electric field reduces as the doping increases till doping concentration reaches 10^{17} cm^{-3} . So, the best design would be a thick low doped p-AlGaIn GR with a field plate.

The Fig. 9 shows the effect of field plating on reducing the peak electric field for the SBD with non-polar p-AlGaIn GR. In Fig. 9, we can see that for doping concentration less than 10^{18} cm^{-3} , in the case of non-polar p-AlGaIn GR, field plating significantly reduces the electric field at the metal edge and the electric field crosses the $\beta\text{-Ga}_2\text{O}_3$ critical electric field of 8 MV/cm at a bias voltage of around 3600 V . For doping concentration above 10^{17} cm^{-3} , the field plating has no effect on reducing the electric field because of shifting of the peak electric field from metal edge to the pn-heterojunction. We can also see that use of a high-k dielectric (HfO_2 , in this case with relative permittivity of 22) with same dimension as the previous case as field plate oxide in conjunction with the guard ring reduces the peak electric field dramatically and the device reaches the $\beta\text{-Ga}_2\text{O}_3$ critical electric field of 8 MV/cm at a reverse bias voltage of 5200 V , which is significantly higher than the highest reported breakdown voltage for any vertical SBD with 10 μm drift layer [33]. The high permittivity difference between the semiconductor and the dielectric generates polarization bound charge inside the dielectric which balances the depletion charge at the semiconductor interface [29], [34], [35]. This charge balance results in flattening of the electric field profile at the dielectric/semiconductor interface reducing its peak magnitude. We have also simulated a field plated SBD with HfO_2 as field plated oxide without a GR and it achieves a breakdown voltage of 4300 V . So, the

use of a GR in conjunction with a field plate increases the breakdown voltage by 900 V compared to the field plated SBD with no GR. We have also analyzed other extreme high-k material such as BaTiO₃ (relative permittivity of 300) as field plate oxide and the breakdown voltage was found to reach 7800 V when used in conjunction with GR. Since BaTiO₃ has no conduction band offset with β -Ga₂O₃, use of BaTiO₃ underneath the metal might cause charge trapping at the dielectric/semiconductor interface. To mitigate the charge trapping, we have analyzed a stacked dielectric of HfO₂ (5 nm)+BaTiO₃ (295 nm). Here the large thickness ratio is used to maintain the high dielectric constant for the series configuration which results in an effective dielectric constant of 248. Using this structure in conjunction with the thick guard ring we are able to get a breakdown voltage of 6200 V.

Among all the devices described the SBD with non-polar p-AlGa_N GR added with field plate and a high-k field plate oxide is found out to be best choice to reduce the electric field. The thick β -Ga₂O₃ epilayers (10 μ m) on (010) β -Ga₂O₃ substrates used in this design can be grown using HVPE and has already been demonstrated [36], [37]. Selective area epitaxy of AlGa_N GRs inside Ga₂O₃ trench pockets can be done using MOCVD [38], [39]. We understand AlGa_N heteroepitaxy on Ga₂O₃ could lead to compromised material quality and will require extensive growth and process optimizations. Experimentally, trench Ga₂O₃ SBDs with field plate structures, were able to achieve FOM as high as 0.95 GW/cm² [33]. Using the concepts explored in this work, if Ga₂O₃ SBDs with GR in conjunction with field plates are implemented, we expect this design to surpass the already high FOM achieved with Ga₂O₃ power SBDs. For instance, with a breakdown voltage of 6200 V and an estimated $R_{ON,SP}$ of 3.55 m Ω -cm², assuming a mobility of 176 cm²/V.s [40], we should be able to achieve extremely high FOM of 10.8 GW/cm².

IV. CONCLUSION

A novel approach to reduce the electric field and thus increasing the breakdown voltage for schottky barrier diode by using p-doped III-nitride guard ring is proposed and shown through a detailed device simulation. This approach circumvents the issue of lack of p-type doping in gallium oxide. The SBD with thick low doped non-polar p-AlGa_N GR in conjunction with a field plate and a high-k dielectric can serve best in terms of reducing the peak electric field. The inclusion of field plate and a high permittivity field plate oxide in case of low doped GR is shown to further reduce the electric field at the metal edges. Further research into the interface properties of the AlGa_N/Ga₂O₃ heterointerface will lead to better understanding and use of such heterojunction-based structures for high performance power electronic devices.

ACKNOWLEDGEMENT

This material is based upon work supported by the Air Force Office of Scientific Research under award number FA9550-18-1-0507 (Program Manager: Dr. Ali Sayir). Any opinions, finding, and conclusions or recommendations expressed in this material are those of the author(s) and do not necessarily reflect the views of the United States Air Force.

REFERENCES

- [1] M. Higashiwaki, K. Sasaki, A. Kuramata, T. Masui, and S. Yamakoshi, "Gallium oxide (Ga₂O₃) metal-semiconductor field-effect transistors on single-crystal β -Ga₂O₃ (010) substrates," *Applied Physics Letters*, vol. 100, no. 1, p. 013504, 2012.
- [2] K. Sasaki, A. Kuramata, T. Masui, E. G. Villora, K. Shimamura, and S. Yamakoshi, "Device-quality β -Ga₂O₃ epitaxial films fabricated by ozone molecular beam epitaxy," *Applied Physics Express*, vol. 5, no. 3, p. 035502, 2012.
- [3] K. Sasaki, M. Higashiwaki, A. Kuramata, T. Masui, and S. Yamakoshi, "Ga₂O₃ Schottky Barrier Diodes Fabricated by Using Single-Crystal β -Ga₂O₃ (010) Substrates," *IEEE electron device letters*, vol. 34, no. 4, pp. 493–495, 2013.
- [4] M. Higashiwaki, K. Sasaki, K. Goto, K. Nomura, Q. T. Thieu, R. Togashi, H. Murakami, Y. Kumagai, B. Monemar, A. Koukitu *et al.*, "Ga₂O₃ Schottky barrier diodes with n-Ga₂O₃ drift layers grown by HVPE," in *2015 73rd Annual Device Research Conference (DRC)*. IEEE, 2015, pp. 29–30.
- [5] K. Konishi, K. Goto, H. Murakami, Y. Kumagai, A. Kuramata, S. Yamakoshi, and M. Higashiwaki, "1-kV vertical Ga₂O₃ field-plated Schottky barrier diodes," *Applied Physics Letters*, vol. 110, no. 10, p. 103506, 2017.
- [6] J. Yang, S. Ahn, F. Ren, S. Pearton, S. Jang, J. Kim, and A. Kuramata, "High reverse breakdown voltage Schottky rectifiers without edge termination on Ga₂O₃," *Applied Physics Letters*, vol. 110, no. 19, p. 192101, 2017.
- [7] K. Sasaki, D. Wakimoto, Q. T. Thieu, Y. Koishikawa, A. Kuramata, M. Higashiwaki, and S. Yamakoshi, "First demonstration of Ga₂O₃ trench MOS-type Schottky barrier diodes," *IEEE Electron Device Letters*, vol. 38, no. 6, pp. 783–785, 2017.
- [8] J. Yang, S. Ahn, F. Ren, S. Pearton, S. Jang, and A. Kuramata, "High Breakdown Voltage (-201) β -Ga₂O₃ Schottky Rectifiers," *IEEE Electron Device Letters*, vol. 38, no. 7, pp. 906–909, 2017.
- [9] J. Yang, F. Ren, M. Tadjer, S. Pearton, and A. Kuramata, "2300 V reverse breakdown voltage Ga₂O₃ schottky rectifiers," *ECS Journal of Solid State Science and Technology*, vol. 7, no. 5, p. Q92, 2018.
- [10] W. Li, Z. Hu, K. Nomoto, Z. Zhang, J.-Y. Hsu, Q. T. Thieu, K. Sasaki, A. Kuramata, D. Jena, and H. G. Xing, "1230 V β -Ga₂O₃ trench Schottky barrier diodes with an ultra-low leakage current of < 1 μ A/cm²," *Applied Physics Letters*, vol. 113, no. 20, p. 202101, 2018.
- [11] W. Li, Z. Hu, K. Nomoto, R. Jinno, Z. Zhang, T. Q. Tu, K. Sasaki, A. Kuramata, D. Jena, and H. G. Xing, "2.44 kV Ga₂O₃ vertical trench Schottky barrier diodes with very low reverse leakage current," in *2018 IEEE International Electron Devices Meeting (IEDM)*. IEEE, 2018, pp. 8–5.
- [12] Y. Wang, Y. Lv, S. Long, X. Zhou, X. Song, S. Liang, T. Han, X. Tan, Z. Feng, S. Cai *et al.*, "High-Voltage (-2 0 1) β -Ga₂O₃ Vertical Schottky Barrier Diode With Thermally-Oxidized Termination," *IEEE Electron Device Letters*, vol. 41, no. 1, pp. 131–134, 2019.
- [13] C.-H. Lin, Y. Yuda, M. H. Wong, M. Sato, N. Takekawa, K. Konishi, T. Watahiki, M. Yamamuka, H. Murakami, Y. Kumagai *et al.*, "Vertical Ga₂O₃ Schottky barrier diodes with guard ring formed by nitrogen-Ion implantation," *IEEE Electron Device Letters*, vol. 40, no. 9, pp. 1487–1490, 2019.
- [14] H. Zhou, Q. Yan, J. Zhang, Y. Lv, Z. Liu, Y. Zhang, K. Dang, P. Dong, Z. Feng, Q. Feng *et al.*, "High-Performance Vertical β -Ga₂O₃ Schottky Barrier Diode With Implanted Edge Termination," *IEEE Electron Device Letters*, vol. 40, no. 11, pp. 1788–1791, 2019.
- [15] Y. Gao, A. Li, Q. Feng, Z. Hu, Z. Feng, K. Zhang, X. Lu, C. Zhang, H. Zhou, W. Mu *et al.*, "High-Voltage β -Ga₂O₃ Schottky Diode with Argon-Implanted Edge Termination," *Nanoscale research letters*, vol. 14, no. 1, p. 8, 2019.
- [16] Q. Zhang, "Semiconductor devices with heterojunction barrier regions and methods of fabricating same," Aug. 25 2015, US Patent 9,117,739.
- [17] M. Muhammed, M. Roldan, Y. Yamashita, S.-L. Sahonta, I. A. Ajia, K. Iizuka, A. Kuramata, C. Humphreys, and I. Roqan, "High-quality III-nitride films on conductive, transparent (-201) oriented β -Ga₂O₃ using a GaN buffer layer," *Scientific reports*, vol. 6, p. 29747, 2016.
- [18] M. M. Muhammed, N. Alwadai, S. Lopatin, A. Kuramata, and I. S. Roqan, "High-Efficiency InGa_N/Ga_N Quantum Well-Based Vertical Light-Emitting Diodes Fabricated on β -Ga₂O₃ Substrate," *ACS applied materials & interfaces*, vol. 9, no. 39, pp. 34 057–34 063, 2017.
- [19] K. Shimamura, E. G. Villora, K. Domen, K. Yui, K. Aoki, and N. Ichinose, "Epitaxial growth of GaN on (1 0 0) β -Ga₂O₃ substrates by metalorganic vapor phase epitaxy," *Japanese Journal of Applied Physics*, vol. 44, no. 1L, p. L7, 2004.

- [20] Y. Cao, R. Li, A. J. Williams, R. Chu, A. L. Corrion, and R. Chang, "Non-polar GaN film growth on (0 1 0) gallium oxide substrate by metal organic chemical vapor deposition," *Journal of Materials Research*, vol. 32, no. 9, pp. 1611–1617, 2017.
- [21] S. Pearton, J. Yang, P. H. Cary IV, F. Ren, J. Kim, M. J. Tadjer, and M. A. Mastro, "A review of Ga₂O₃ materials, processing, and devices," *Applied Physics Reviews*, vol. 5, no. 1, p. 011301, 2018.
- [22] I. Vurgaftman, J. á. Meyer, and L. á. Ram-Mohan, "Band parameters for III-V compound semiconductors and their alloys," *Journal of applied physics*, vol. 89, no. 11, pp. 5815–5875, 2001.
- [23] M. E. Levinshtein, S. L. Rumyantsev, and M. S. Shur, "Properties of advanced semiconductor materials : GaN, AlN, InN, BN, SiC, SiGe," 2001.
- [24] A. Bhattacharyya, P. Ranga, M. Saleh, S. Roy, M. A. Scarpulla, K. G. Lynn, and S. Krishnamoorthy, "Schottky Barrier Height Engineering In β -Ga₂O₃ Using SiO₂ Interlayer Dielectric," *IEEE Journal of the Electron Devices Society*, pp. 1–1, 2020.
- [25] *Sentaurus Device User Manual, (Version N-2017.09, March 2017)*.
- [26] W. Wei, Z. Qin, S. Fan, Z. Li, K. Shi, Q. Zhu, and G. Zhang, "Valence band offset of β -Ga₂O₃/wurtzite GaN heterostructure measured by X-ray photoelectron spectroscopy," *Nanoscale research letters*, vol. 7, no. 1, p. 562, 2012.
- [27] M. Xiao, R. Zhang, D. Dong, H. Wang, and Y. Zhang, "Design and Simulation of GaN Superjunction Transistors With 2-DEG Channels and Fin Channels," *IEEE Journal of Emerging and Selected Topics in Power Electronics*, vol. 7, no. 3, pp. 1475–1484, Sep. 2019.
- [28] Y. Zhang, M. Sun, Z. Liu, D. Piedra, H.-S. Lee, F. Gao, T. Fujishima, and T. Palacios, "Electrothermal simulation and thermal performance study of GaN vertical and lateral power transistors," *IEEE Transactions on Electron Devices*, vol. 60, no. 7, pp. 2224–2230, 2013.
- [29] Z. Xia, C. Wang, N. K. Kalarickal, S. Stemmer, and S. Rajan, "Design of Transistors Using High-Permittivity Materials," *IEEE Transactions on Electron Devices*, vol. 66, no. 2, pp. 896–900, 2019.
- [30] M. J. Tadjer, J. L. Lyons, N. Nepal, J. A. Freitas, A. D. Koehler, and G. M. Foster, "Review Theory and Characterization of Doping and Defects in β -Ga₂O₃," *ECS Journal of Solid State Science and Technology*, vol. 8, no. 7, pp. Q3187–Q3194, 2019.
- [31] M. A. Reshchikov, P. Ghimire, and D. O. Demchenko, "Magnesium acceptor in gallium nitride. I. Photoluminescence from Mg-doped GaN," *Phys. Rev. B*, vol. 97, p. 205204, May 2018.
- [32] J. Simon, V. Protasenko, C. Lian, H. Xing, and D. Jena, "Polarization-induced hole doping in wide-band-gap uniaxial semiconductor heterostructures," *Science*, vol. 327, no. 5961, pp. 60–64, 2010.
- [33] W. Li, K. Nomoto, Z. Hu, D. Jena, and H. G. Xing, "Field-Plated Ga₂O₃ Trench Schottky Barrier Diodes With a BV²/R_{on,sp} of up to 0.95 GW/cm²," *IEEE Electron Device Letters*, vol. 41, no. 1, pp. 107–110, Jan 2020.
- [34] S. Rajan, Z. Xia, and C. Wang, "Dielectric passivation for electronic devices," Jan. 2 2020, US Patent App. 16/455,736.
- [35] T. Kabemura, S. Ueda, Y. Kawada, and K. Horio, "Enhancement of Breakdown Voltage in AlGaIn/GaN HEMTs: Field Plate Plus High-*k* Passivation Layer and High Acceptor Density in Buffer Layer," *IEEE Transactions on Electron Devices*, vol. 65, no. 9, pp. 3848–3854, 2018.
- [36] H. Murakami, K. Nomura, K. Goto, K. Sasaki, K. Kawara, Q. T. Thieu, R. Togashi, Y. Kumagai, M. Higashiwaki, A. Kuramata *et al.*, "Homoepitaxial growth of β -Ga₂O₃ layers by halide vapor phase epitaxy," *Applied Physics Express*, vol. 8, no. 1, p. 015503, 2014.
- [37] J. Leach, K. Udway, J. Rumsey, G. Dodson, H. Splawn, and K. Evans, "Halide vapor phase epitaxial growth of β -Ga₂O₃ and α -Ga₂O₃ films," *APL Materials*, vol. 7, no. 2, p. 022504, 2019.
- [38] D. Kapolnek, S. Keller, R. Vetury, R. Underwood, P. Kozodoy, S. Den Baars, and U. Mishra, "Anisotropic epitaxial lateral growth in GaN selective area epitaxy," *Applied Physics Letters*, vol. 71, no. 9, pp. 1204–1206, 1997.
- [39] Y. Kawaguchi, Y. Honda, H. Matsushima, M. Yamaguchi, K. Hiramatsu, and N. Sawaki, "Selective Area Growth of GaN on Si Substrate Using SiO₂ Mask by Metalorganic Vapor Phase Epitaxy," *Japanese journal of applied physics*, vol. 37, no. 8B, p. L966, 1998.
- [40] Y. Zhang, F. Alema, A. Mauze, O. S. Koksaldi, R. Miller, A. Osinsky, and J. S. Speck, "MOCVD grown epitaxial β -Ga₂O₃ thin film with an electron mobility of 176 cm²/V s at room temperature," *APL Materials*, vol. 7, no. 2, p. 022506, 2019.